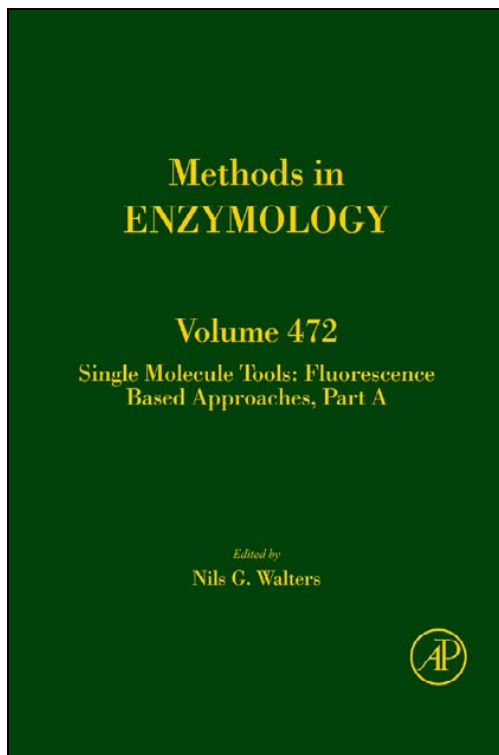


**Provided for non-commercial research and educational use only.  
Not for reproduction, distribution or commercial use.**

This chapter was originally published in the book *METHODS IN ENZYMOLOGY*, Vol. 472, published by Elsevier, and the attached copy is provided by Elsevier for the author's benefit and for the benefit of the author's institution, for non-commercial research and educational use including without limitation use in instruction at your institution, sending it to specific colleagues who know you, and providing a copy to your institution's administrator.



All other uses, reproduction and distribution, including without limitation commercial reprints, selling or licensing copies or access, or posting on open internet sites, your personal or institution's website or repository, are prohibited. For exceptions, permission may be sought for such use through Elsevier's permissions site at: <http://www.elsevier.com/locate/permissionusematerial>

From: Arjun Raj and Sanjay Tyagi, Detection of Individual Endogenous  
RNA Transcripts in Situ Using Multiple Singly Labeled Probes  
In Nils G. Walters editor: *METHODS IN ENZYMOLOGY*, Vol. 472,  
Burlington: Academic Press, 2010, pp.365-386.  
ISBN: 978-0-12-374954-3  
© Copyright 2010, Elsevier Inc.  
Academic Press.

# DETECTION OF INDIVIDUAL ENDOGENOUS RNA TRANSCRIPTS *IN SITU* USING MULTIPLE SINGLY LABELED PROBES

Arjun Raj<sup>★</sup> and Sanjay Tyagi<sup>†</sup>

## Contents

|   |     |
|---|-----|
| 1. Introduction   | 366 |
| 2. Design and Synthesis of Fluorescent Oligonucleotide Probe Sets | 369 |
| 2.1. Design   | 369 |
| 2.2. Synthesis and purification                                   | 369 |
| 3. Preparation of Samples for <i>In Situ</i> Hybridization        | 373 |
| 3.1. Fixation solutions   | 373 |
| 3.2. Fixation protocols   | 375 |
| 4. Hybridization  | 377 |
| 4.1. Hybridization solutions                                      | 378 |
| 4.2. Hybridization protocols                                      | 379 |
| 5. Imaging  | 381 |
| 5.1. Microscopy equipment   | 381 |
| 6. Image Analysis   | 384 |
| Acknowledgments   | 386 |
| References  | 386 |

## Abstract

Measurements of gene expression within single cells have revealed startling variability otherwise hidden in bulk measurements. Here, we present an *in situ* hybridization method capable of detecting individual mRNA molecules, thus permitting the accurate quantification and localization of mRNA within fixed sample. Our *in situ* protocol involves probing the target mRNA using a series of singly labeled oligonucleotide probes. This method is simple to implement and is applicable to a variety of biological samples. We also discuss some aspects of image processing required for analyzing the resulting data.

<sup>★</sup> Department of Bioengineering, University of Pennsylvania, Philadelphia, Pennsylvania, USA

<sup>†</sup> Public Health Research Institute, New Jersey Medical School-UMDNJ, Newark, New Jersey, USA



## 1. INTRODUCTION

Single cell measurements have revealed that gene expression in individual cells can deviate significantly from the average behavior of cell populations, with significant biological consequences (Larson *et al.*, 2009; Maheshri and O'Shea, 2007; Raj and Van Oudenaarden, 2008, 2009; ). These findings have created a need for accurate methods of quantifying expression in single cells, ideally even yielding intracellular spatial information about the localization of mRNAs.

A natural candidate for such a method is *in situ* hybridization, in which labeled nucleotide probes find their specific targets through Watson–Crick base pairing (Levsky and Singer, 2003). Initially, researchers performed *in situ* hybridizations using radioactive probes (Gall, 1968). Early improvements involved linking the probes to enzymes that catalyze chromogenic or fluorogenic reactions (Raap *et al.*, 1995; Tautz and Pfeifle, 1989). Unfortunately, these reactions generated molecules that diffused away from the probe itself, making it difficult to ascertain the precise spatial location of the target. Alternatively, one could use fluorescently labeled probes, thus sidestepping the issues of localization, but the sensitivity of such methods was relatively poor.

Singer and colleagues then developed an *in situ* hybridization procedure that was both sensitive enough to permit the detection of single mRNA molecules, but also restricted the fluorescence to reside close to the target (Femino *et al.*, 1998). Their method involved the use of five 50mer DNA oligonucleotides, each of which was conjugated to five fluorophore moieties. The authors convincingly demonstrated single molecule sensitivity, with spots corresponding to individual mRNA molecules, and their method has seen subsequent use (Maamar *et al.*, 2007; Zenklusen *et al.*, 2008). However, they estimated that over 30% of the transcripts hybridized to either zero (5%) or to just one (25%) of the oligonucleotide probes (Table 1 of supplementary information in Femino *et al.* (1998)). This lack of coupling efficiency is worrisome because the detection of just a single probe cannot discriminate between legitimate binding to the target and nonspecific binding. Another issue with this method is that the probes are generally difficult to generate: it is difficult to efficiently label DNA oligonucleotides with multiple fluors, and each probe must be synthesized and purified individually.

Our method involves probing target mRNAs using a larger number (> 30) of shorter oligonucleotides (20 bases), each of which hybridize to a different portion of the target mRNA (Fig. 17.1). We label each of these oligonucleotides with a single fluorophore at its 3' end; thus, upon hybridization, a large number of fluors are all brought within close proximity of

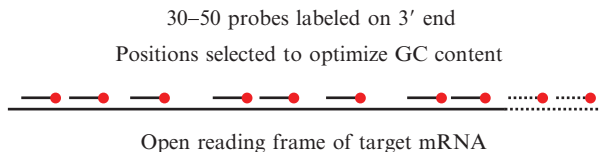


**Figure 17.1** Depiction of scheme for imaging individual mRNA molecules using singly labeled oligonucleotide probes. The placement of the probes is often nonuniform in order to maintain an optimal GC content for all probes, thus matching hybridization conditions between probes. See [Raj \*et al.\* \(2008\)](#) for all sequences used in this chapter.

the target. The presence of so many fluorophores in a single location results in enough fluorescence that the spot can be made out as a diffraction-limited spot in a widefield fluorescence microscope. Our method achieves its specificity and sensitivity owing to the large number of probes used. The rate of false negatives is low because even if the target RNA molecule has been partly degraded or is partly obscured by RNA binding proteins, at least some fraction of the probes will still bind to it, yielding a detectable signal. The rate of false positives is also low because one only detects a signal when a significant fraction of the probes are bound. Thus, off-target binding of individual probes will not yield much signal above background. Such false positives are particularly a concern in other methods consisting of the hybridization of a single probe followed by an enzymatic signal amplification; in such cases, it is impossible to distinguish a single nonspecific binding event from a legitimate interaction.

Moreover, our method is straightforward and easy to implement, owing to the simplicity of the chemistries involved. Advances in oligonucleotide synthesis make it cost effective to purchase large numbers of singly functionalized probes, and the labeling procedure can be performed on a pooled set of these oligonucleotides, greatly reducing the effort required. Another feature of our method is that it can be combined with other methods like DNA FISH ([Vargas \*et al.\*, 2005](#)) ([Arjun Raj unpublished observations](#)) and immunofluorescence ([Raj \*et al.\*, 2008](#)). Furthermore, the fact that we see diffraction-limited spots allows us to precisely determine the location of the center of the spot beyond the optical diffraction limit ([Yildiz \*et al.\*, 2003](#)), technically making our method a version of super-resolution imaging.

One question that often arises is how we know that each fluorescent spot represents a single RNA molecule rather than a conglomeration of multiple target mRNAs. We have several pieces of evidence supporting the conclusion that each spot corresponds to a single RNA, mostly outlined in [Vargas \*et al.\* \(2005\)](#). In one experiment, we synthesized mRNAs prehybridized with two different fluorophores (effectively, we made “red” and “green” mRNAs). We then injected a mixture of these red

and green mRNAs into single cells. If the mRNAs were in fact clumping, the spots would have contained both red and green mRNAs and would thus appear yellow. What we found, however, was that each spot was either red or green but never both, showing that each spot corresponded to individual red or green mRNA molecules. Moreover, the signal intensities from these synthetic mRNAs were roughly identical to those from endogenously transcribed mRNAs, indicating that endogenously transcribed mRNAs also do not form clumps. It is possible, of course, that certain other mRNAs form clumps, and a formal proof requires this procedure be followed for each particular mRNA under study, but at least this case is consistent with the null hypothesis that mRNAs do not form conglomerates.

Another piece of evidence comes from examining the distribution of spot intensities (Raj *et al.*, 2008; Vargas *et al.*, 2005). If some of the spots were conglomerates of small numbers of mRNA, one would expect that some spots would consist of one mRNA, some of two, and so on. The distribution of spot intensities would then show multiple peaks, as observed with MS2 binding-site-tagged mRNAs, which are known to clump (Golding *et al.*, 2005). Instead, we always see a single peak (Raj *et al.*, 2008; Vargas *et al.*, 2005), consistent with each spot representing single mRNA molecules.

We also compared mRNA counts obtained with our method (specifically, average number of mRNA per cell) to those obtained by quantitative RT-PCR and found that the results compared favorably, coming within 30% of each other. These measurements not only bolster our claim to be detecting individual molecules, but also show that our fixation procedure does not result in the loss of a significant fraction of the mRNAs in the sample.

Another potential issue could be the occlusion of the target RNA by various RNA-binding proteins; for example, cytoplasmic mRNAs being occluded by ribosomes. We doubt this factor is significant, though, partly because of the quantitative RT-PCR experiments described above. Also, we simultaneously labeled both the open-reading frame and the 3' UTR (upon which there should be no ribosomes) simultaneously but with differently colored probes, and we found a high degree of colocalization (80%), showing that at least ribosome binding is not a significant impediment to RNA detection.

In this chapter, we describe the procedures involved in detecting individual RNA molecules *in situ*. These are (1) designing and synthesizing the fluorescently labeled oligonucleotides, (2) fixation of the biological specimen, (3) hybridization, (4) imaging on a fluorescence microscope, and (5) data analysis. None of these steps utilize any exotic chemicals, procedures or equipment, and we will indicate as needed any aspects of the application of our method that require any special attention.



## 2. DESIGN AND SYNTHESIS OF FLUORESCENT OLIGONUCLEOTIDE PROBE SETS

### 2.1. Design

Our method involves the synthesis of a set of fluorescently labeled oligonucleotides (which we call the “probe set”) that will hybridize along the length of target RNA molecule. There are a few general guidelines we typically follow when designing these oligonucleotides. Firstly, the probe sets typically consist of anywhere between 30 and 96 (typically 48) different 20mer DNA oligonucleotides, each complementary to a different region of the target RNA, with no less than two bases separating any two oligonucleotides (Fig. 17.1). We have found that one can sometimes obtain signals with less than 30 oligonucleotides, but the signals are often fainter. Forty-eight probes appear to be sufficient to generate a robust signal in most instances, and many synthesis companies sell parallel orders of oligonucleotides in batches of 48, which is why that is the default number of oligonucleotides we utilize in our probe sets.

Another issue is that of the GC content of the individual oligonucleotides. Given that GC content can significantly alter the hybridization parameters, we consider it desirable to make the GC contents of the various oligonucleotides as uniform as possible, thus ensuring that as many probes as possible will bind at a given hybridization stringency. In order to design such probe sets, we have deployed a web-based program (<http://www.singlemoleculefish.com>) that, given a target RNA sequence, a desired number of probes and a target GC percentage, will generate a set of oligonucleotides whose GC contents are as uniform as possible. Of course, for shorter target RNAs, there is a tradeoff between the number of probes one can generate and the GC uniformity of those probes, but we have not systematically studied these effects. Anecdotally, we find that beyond around 35 probes, optimizing the GC content of the probes is probably more useful than squeezing more probes onto the target mRNA. As reference points, we note that we have seen decent signals using as few as 20 probes and excellent signals using just 30 probes, meaning that one can detect mRNAs as short as  $\sim 500$  bases.

### 2.2. Synthesis and purification

Once the oligonucleotide sequences are generated, we order the oligonucleotides synthesized with a 3' amine group, which we use for coupling the fluorophore. The oligonucleotides we order are desalted and resuspended in water rather than TE, since Tris can interfere with subsequent amine-coupling reactions. Since the amount of oligonucleotide used for each hybridization is typically very small, one should have the oligonucleotides

synthesized on the smallest scale possible. We order our oligonucleotides from Biosearch Technologies (Novato, CA) at a scale of 10 nmol per oligo, which are delivered to us in 100  $\mu$ l of water. We have found that other means of labeling oligonucleotides (especially internal amino-dTs) have far lower coupling efficiencies.

The next step is to couple the oligonucleotides to the desired fluorophore. We utilize succinimidyl ester derivatives to couple to the amine group at the 3' end of the oligonucleotides (we will discuss the choice of fluorophore shortly). Rather than coupling and purifying each oligonucleotide individually, we instead couple and purify the oligonucleotides *en masse* via reverse phase HPLC, significantly reducing the labor involved:

1. Combine the uncoupled oligonucleotides by pooling 1 nmole of each oligonucleotide (10  $\mu$ l in our case) together.
2. Add enough volume of 1 M sodium bicarbonate (pH 8.0) so that the oligonucleotide pool contains 0.1 M sodium bicarbonate.
3. Meanwhile, dissolve the fluorophore in 50  $\mu$ l of 0.1 M sodium bicarbonate (pH 8.0). Note that some fluorophores, such as tetramethylrhodamine (TMR), are more readily soluble in organic solvents; we first dissolve those fluorophores in around 5  $\mu$ l of DMSO and then add 50  $\mu$ l of 0.1 M sodium bicarbonate.
4. Add the fluorophore solution to the oligonucleotide solution.
5. Let the reaction sit in the dark overnight at room temperature.

At this point, the tube will contain uncoupled fluorophore, uncoupled oligonucleotides, and coupled oligonucleotides. In order to remove the uncoupled fluorophores, we perform an ethanol (EtOH) precipitation:

6. Add 0.13 vol of 3 M sodium acetate (pH 5.2) and 2.5 vol EtOH to the reaction.
7. Store at  $-80^{\circ}\text{C}$  for at least 1 h.
8. Spin in a  $4^{\circ}\text{C}$  microcentrifuge at maximum speed for 15 min. A colored pellet containing the coupled and uncoupled oligonucleotides should form at the bottom of the tube.
9. Carefully pipette off as much of the supernatant as possible. This supernatant contains the uncoupled fluorophore.

In order to separate the uncoupled oligonucleotides from the coupled oligonucleotides, we purify the oligonucleotides by HPLC. The typically hydrophobic organic fluorophores cause a large increase in hydrophobicity of the coupled oligonucleotides as compared to the rather hydrophilic uncoupled oligonucleotides. The size of this increase is much larger than the variation in the hydrophobicity of the individual oligonucleotides, thus enabling us to purify the entire pool of oligonucleotides at once.

This procedure requires an HPLC equipped with a C18 column (C18TP104) and a dual wavelength detector (or diode array detector) set to

detect DNA absorption (260 nm) as well as the absorption of the coupled fluorophore (e.g., 555 nm for TMR). We have found it easiest to collect the desired fractions manually rather than automatically from the outflow. For our gradient, we use 0.1 M Triethyl ammonium acetate, pH 6.5 (Buffer A) and acetonitrile, pH 6.5 (Buffer B), ranging from 7% to 30% Buffer B over the course of 30 min at a flow rate of 1 mL per min (after this, be sure to run the column at 70% Buffer B for 10 min in order to clear the column of extraneous molecules and then equilibrate the column at 7% Buffer B for 10 min before running another sample). The specific gradient may depend on the exact nature of your HPLC setup, but should be at least similar to that we describe here.

While the gradient is running, continuously monitor the absorption in the 260 and 555 nm channels. Initially, you will see a large set of peaks at 260 nm while the 555 nm absorption remains low. This peak contains the uncoupled oligonucleotide. After that peak passes, you will observe another set of peaks in which there is large absorption in both the 260 and 555 nm channels (Fig. 17.2). This peak contains the coupled oligonucleotides. Collect this fraction as it passes through the HPLC (the total volume collected will typically be between 2 and 6 mL). Be sure to collect the entire peak rather than just the “top.” This is important, because different parts of the peak will contain different oligonucleotides. It also bears mentioning that even labeled oligonucleotide can generate multiple peaks due to incomplete deprotection or dye-induced chemical variation. We do not think, though, that these issues lead to any serious problems in oligonucleotide purity.

Once the fraction is collected, dry the samples in a lyophilizer or a speedvac rated for use with acetonitrile, then resuspend the fractions in 50–100  $\mu$ L of Tris EDTA (TE), pH 8.0. This is the stock of your probe (concentration of roughly 0.1–1  $\mu$ M) from which you can make working dilutions (1:10, 1:20, 1:50, 1:100) for your hybridizations.

As for the choice of fluorophore, the ones we commonly use are TMR (Molecular Probes, Invitrogen), Alexa 594 (Molecular Probes, Invitrogen), and Cy5 (GE Amersham). Using appropriate filter sets (Table 17.1), we are able to independently image these three colors reliably in most samples we have examined with no bleedthrough between channels (Fig. 17.3). While it is possible that one can use fluorophores that absorb and emit at even shorter wavelengths (e.g., Alexa 488), we have found that background autofluorescence at these wavelengths is usually strong enough that it is difficult to make out the signals (although we have had success with Alexa 488 on occasion). Even the signals from TMR and to some extent Alexa 594 are sometimes marred by autofluorescent blobs that make the particles hard to distinguish. In such situations, one can get some idea of whether or not the signals are real by taking pictures of the sample using GFP/fluorescein filters—background autofluorescence typically has a broad emission spectrum and will often show up in multiple channels, whereas the organic dyes will not appear in the GFP channel. Reducing this background is often



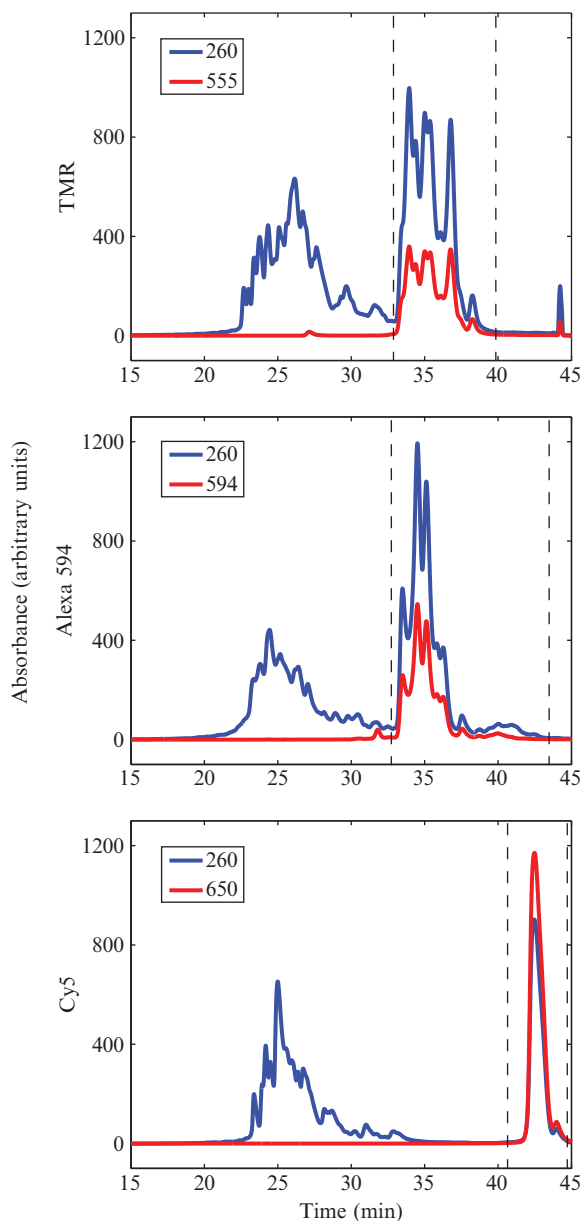


**Figure 17.2** Sample HPLC chromatographs showing absorbance at 260 nm (blue) and 555, 594, and 650 nm (red; TMR, Alexa 594, and Cy5, respectively). The first 260 nm peak is the uncoupled oligonucleotides. The next peak appears in both the 260 nm and fluorophore absorbance channels, indicating that this is the coupled oligonucleotides. Collect the entire fraction between the gray dotted lines.

**Table 17.1** Optical filters for multiplex mRNA detection

|           | Excitation | Dichroic | Emission  | Supplier |
|-----------|------------|----------|-----------|----------|
| TMR       | 546DF10    | 555DRLP  | 580DF30   | Omega    |
| Alexa 594 | 590DF10    | 610DRLP  | 630DF30   | Omega    |
| Cy5       | HQ620/60x  | Q660LP   | HQ700/75m | Chroma   |

Details of the excitation, dichroic, and emission filters used for multiplex detection with TMR, Alexa 594, and Cy5. The nomenclature used is specific to the suppliers listed on the right (Omega Optical, Chroma). The first and second numbers refer to the center and width of the bandpass region, respectively.

difficult and is very sample dependent, with some cell lines and tissues exhibiting high levels of background, often related to cellular stress.

Another factor to consider is the fact that Alexa 594 and especially TMR are fairly photostable and thus require no special care to be taken about photobleaching when imaging. Cy5, on the other hand, is notorious for being rapidly photobleached. In order to combat this, we use a glucose-oxidase (glox)-based oxygen scavenging mounting medium (described later in this chapter; adapted from Yildiz *et al.*, 2003), which reduces the photobleaching rate of Cy5 to levels comparable to that of TMR. Given the low autofluorescent background at these far red wavelengths, Cy5 is an excellent choice for samples in which reduction in cellular autofluorescence is impossible.

### 3. PREPARATION OF SAMPLES FOR *IN SITU* HYBRIDIZATION

In this section, we outline the procedures for fixation and permeabilization of various biological samples for use in *in situ* hybridization. These protocols are based on the protocols developed in the lab of Robert Singer (Femino *et al.*, 1998; <http://www.singerlab.org/protocols>). While the specifics may change slightly from organism to organism, the fundamental procedure is roughly the same in all cases: fix the sample in 3.7% (v/v) formaldehyde (i.e., 10% formalin) in 1× phosphate buffered saline (PBS), then permeabilize in 70% ethanol, at which point samples can be stored at 4 °C for weeks (even months) without degradation. Note that all solutions used postfixation should be made with nuclease-free water.

#### 3.1. Fixation solutions

##### 3.1.1. Fixation solution (3.7% formaldehyde/10% formalin, 1× PBS)

- 40 mL RNase free H<sub>2</sub>O (Ambion)
- 5 mL 37% (v/v) formaldehyde (100% formalin)
- 5 mL 10× PBS (RNase free, Ambion)

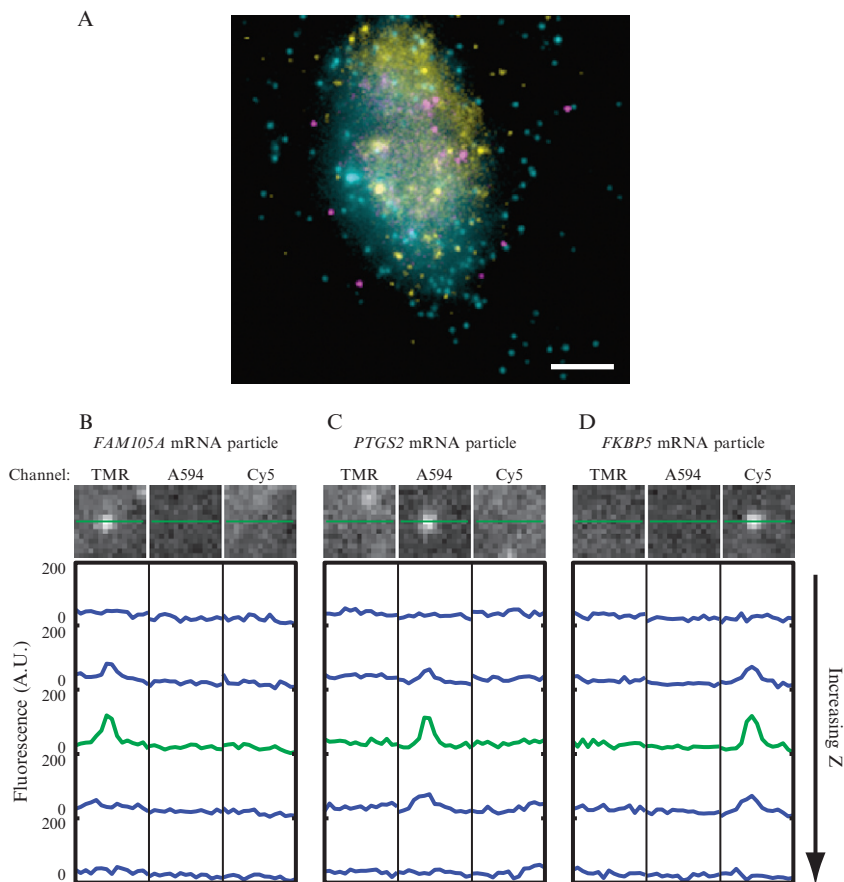


**Figure 17.3** Demonstration of three color mRNA detection. (A) Expression of FKBP5 (blue), PTGS2 (purple), and FAM105A (yellow) mRNAs in human carcinoma cell line A549. Scale bar is 5  $\mu\text{m}$  long. (B–D) Examination of fluorescent spot bleed-through. (B) Images of an FAM105A mRNA spot labeled with TMR as seen through the TMR, Alexa 594, and Cy5 filter channels. Linescans of fluorescent intensity corresponding to the line through the image are given below, with the different linescans corresponding to measurements taken at increasing  $z$  (0.25  $\mu\text{m}$  spacing). The green linescan corresponds to the  $z$ -slice shown in the image itself. A similar analysis was performed for a PTGS2 mRNA spot labeled with Alexa 594 (C) and an FKBP5 mRNA particle labeled with Cy5 (D). All linescan intensity measurements had the camera background subtracted but range between 0 and 200 arbitrary fluorescence units.

### 3.1.2. Buffer B (1.2 M sorbitol, 0.1 M Potassium phosphate)

218 g sorbitol

17.4 g Potassium phosphate (dibasic)

RNase free water to 1 L

### 3.1.3. Spheroplasting buffer

10 mL Buffer B

100  $\mu$ L 200 mM vanadyl ribonucleoside complex (New England Biolabs)

### 3.1.4. M9

5.8 g  $\text{Na}_2\text{HPO}_4$

3.0 g  $\text{KH}_2\text{PO}_4$

0.5 g NaCl

1.0 g  $\text{NH}_4\text{Cl}$

Double-distilled  $\text{ddH}_2\text{O}$  ( $\text{ddH}_2\text{O}$ ) to 1 L

## 3.2. Fixation protocols

### 3.2.1. Fixation of yeast cells

1. Grow yeast to an optical density (OD, at 260 nm) of around 0.1–0.2 in a 45-mL volume of minimal media.
2. Add 5-mL of 37% (v/v) formaldehyde directly to growth media and let sit for 45 min.
3. Wash 2 $\times$  twice with 10 mL ice-cold Buffer B.
4. Add 1 mL of spheroplasting buffer, transferring to a microcentrifuge tube.
5. Add 1  $\mu$ L of zymolyase and incubate at 30  $^\circ\text{C}$  for 15 min.
6. Wash 2 $\times$  twice with 1 mL ice-cold Buffer B, spinning at low speed ( $\sim$ 2000 rpm).
7. Add 1 mL of 70% (v/v) EtOH and leave at least overnight at 4  $^\circ\text{C}$ .

### 3.2.2. Fixation of adherent mammalian cells

1. Grow cells on #1 coverglasses set in six-well culture dishes or in Lab-Tek chambered coverglass (with #1 coverglass on the bottom; we have had bad results with #1.5 coverglass).
2. Aspirate growth medium.
3. Wash with 1 $\times$  PBS.
4. Add fixation solution and incubate at room temperature for 10 min.
5. Wash 2 $\times$  twice with 1 $\times$  PBS.
6. Add 70% (v/v) EtOH and store at 4  $^\circ\text{C}$  at least overnight.

### 3.2.3. Fixation of *Caenorhabditis elegans* larvae (L1–L4)

1. Grow larvae in a plate seeded with OP50.
2. Add 5 mL M9 buffer and swirl in plate to release worms from surface, then move worms to a 15 mL conical centrifuge tube.

We often use DI water instead of M9 in this step and in step 4 and get fine results.

3. Spin down worms and aspirate.
4. Wash with 5 mL M9 buffer.
5. Spin down worms and aspirate.
6. Add 1 mL fixation solution, transfer to microcentrifuge tube, and incubate for 45 min.
7. Wash 2× with 1 mL 1× PBS.
8. Resuspend in 1 mL of 70% EtOH and leave for at least overnight at 4 °C. We have sporadic reports that longer incubations at 4 °C in EtOH (i.e., 5 days) can reduce autofluorescence, but we do not think it really matters.

### 3.2.4. Fixation of *C. elegans* embryos

1. Add 5 mL M9 buffer to a plate of gravid hermaphrodites and swirl to release worms from surface. Move worms to a 15-mL conical centrifuge tube.

We often use DI water instead of M9 in this and subsequent steps and get fine results.

2. Spin down and add bleaching solution (40 mL H<sub>2</sub>O, 7.2 mL 5 N NaOH, 4.5 mL 6% NaHOCl).
3. Vortex for roughly 4–8 min until worms disappear and only embryos remain.
4. Spin down and aspirate, then wash 2× twice in M9 buffer.
5. Resuspend in 1-mL fixation solution and incubate at room temperature for 15 min.
6. Vortex and then immediately submerge tube in liquid nitrogen for 1 min to freeze crack the embryos' eggshells.
7. Thaw in water at room temperature.
8. Once thawed, vortex and place on ice for 20 min.
9. Wash twice with 1 mL 1× PBS.
10. Resuspend in 1 mL of 70% (v/v) EtOH and store at least overnight at 4 °C.

### 3.2.5. Fixation of *Drosophila melanogaster* wing imaginal discs

1. Submerge 3rd instar larvae in 1 mL 1× PBS and dissect to release wing imaginal discs.
2. Place discs at the bottom of a chambered coverglass. They should stick readily.

3. Fix wing discs by aspirating PBS and adding 1 mL fixation solution; incubate at room temperature for 45 min.
4. Wash 2× twice with 1 mL 1× PBS to remove fixative.
5. Add 1 mL of 70% EtOH and leave at least overnight at 4 °C.

### 3.2.6. Fixation of tissue sections

1. Freeze tissue section in optimal cutting temperature compound (OCT). We have heard reports that using sucrose-based cryoprotectants can lead to high background and so should be avoided.
2. Slice the tissue section into 4–10 micron sections using a cryotome and affix the sections to #1 coverslips; the sections can then be stored for months at –80 °C.

*Notes:* Although it is a more standard procedure, do not affix the tissue sections to slides, as this greatly hinders the visualization of the fluorescent spots. Also, the use of poly-L-lysine or some similar surface treatment may enhance the degree to which your tissue section sticks to the coverglass.

3. Thaw the section and immediately fix in fixation solution, either in a coplin jar or a six-well plate.

*Note:* we perform this procedure by affixing a perfusion chamber (Grace Biolabs) to a 24-mm × 50-mm coverglass and adding all solutions, etc. to this chamber. Using the perfusion chamber greatly reduces the amount of fixing/washing reagents required.

4. Wash twice with 1 mL 1× PBS to remove fixative.
5. Add 1 mL of 70% (v/v) EtOH and leave for 1 h at room temperature.

*Note:* some researchers have reported trouble with their sections floating off of the coverslip when stored for prolonged periods of time in 70% EtOH; thus, we recommend beginning the *in situ* hybridization less than 1 h following fixation.

## 4. HYBRIDIZATION

Hybridization consists of a brief prehybridization followed by an overnight hybridization with the oligonucleotide probes. In the morning, two washes in a washing buffer remove the nonhybridized probes and the samples are essentially ready for imaging. There are three basic parameters involved in the hybridization. One is the concentration of the probes used in the hybridization. We typically determine the appropriate concentration empirically, but we have found that (generally) a concentration in the vicinity of 5–50 nM works. Moreover, we have found that there is a fairly

significant range (roughly a factor of 2 or 3 in either direction) of concentrations over which the signals are similar and readily quantifiable. When possible, it is best to optimize the probe concentration rather than changing other factors in the hybridization, since multiplex detection requires shared hybridization conditions, which are easy to match when the only variable is different concentrations of probes. The other two parameters of the hybridization are related and concern the stringency of the hybridization itself: one is the temperature at which one hybridizes the probes, and the other is the concentration of formamide used in the hybridization and washes. Regarding the former, higher temperature generally leads to higher stringency, as fewer of the probes will bind (nonspecifically or specifically) as the temperature increases. We typically use either 30 °C or room temperature, but rarely change this variable, especially since changing the formamide concentration is largely equivalent and is easier to control in a fine-grained manner. To adjust the stringency via formamide, the main point is that the higher the concentration of formamide, the higher the stringency. We typically use 10% (v/v) for most of our hybridizations, but sometimes probes with GC contents of 55–60% require the use of 25% (v/v) formamide. It is important, however, to note that more stringent conditions can lead to a dramatic rate of false negatives: one can only see a few faint looking spots, when in reality, there are many more mRNAs present. Thus, it is generally better to begin with the less stringent 10% conditions and then work up from there. Also, we have found that adding some wet paper towels in the hybridization chamber is NOT helpful and often causes a spot-like background.

## 4.1. Hybridization solutions

### 4.1.1. Hybridization buffer (10 mL)

Dextran sulfate (1 g)

*Escherichia coli* tRNA (10 mg)

Vanadyl ribonucleoside complex (NEB) (100  $\mu$ L of 200 mM stock)

BSA (RNase free) (Ambion) (40  $\mu$ L of 5 mg/mL)

20 $\times$  SSC (nuclease free, Ambion) (1 mL)

Formamide (deionized, Ambion) (1 mL for 10% final concentration, can increase formamide to increase stringency)

Nuclease free (NF) water (Ambion) (to 10 mL final volume)

First, mix the dextran sulfate in about 4 mL of water with gentle agitation at room temperature until dissolved (can take min to h, depending on the batch). Then add the other components. We then keep the hybridization solution in 0.5 mL aliquots at  $-20^{\circ}\text{C}$ .

#### 4.1.2. Wash buffer (50 mL):

Wash/prehybridization buffer:

- 40 mL RNase free water (Ambion)
- 5 mL Formamide (deionized, Ambion)
- 5 mL 20× SSC (RNase free, Ambion)

*Note:* one can increase the stringency by increasing the amount of formamide.

#### 4.1.3. Antifade buffer and enzymes:

- 10% (w/v) glucose in nuclease free water
- 2 M Tris-HCl, pH 8.0
- 20× SSC (Ambion)
- Nuclease free water (Ambion)
- Glox (Sigma) (diluted to 3.7 mg/mL stock in 50 mM sodium acetate, pH ~5)
- Catalase (Sigma)

Mix together 0.85 mL of NF water and add 100  $\mu$ L of 20× SSC, 40  $\mu$ L of 10% (w/v) glucose and 5  $\mu$ L of 2 M Tris-HCl. Vortex and then transfer 100  $\mu$ L of this “glox” buffer to another tube, to which one should add 1  $\mu$ L of glox stock and 1  $\mu$ L of (nicely vortexed) catalase suspension. The remainder will be used as an equilibration buffer.

## 4.2. Hybridization protocols

### 4.2.1. Hybridization in solution

1. Prepare the hybridization solution: to 100  $\mu$ L of hybridization buffer, add 1–3  $\mu$ L of probe at the appropriate concentration, then vortex and centrifuge.
  - a. Be sure to warm the hybridization solution to room temperature before opening it.
  - b. For the initial test of a set of probes, it is best to start four separate hybridization reactions by adding 1  $\mu$ L each of the 1:10, 1:20, 1:50, and 1:100 working dilutions of probes to see which one is optimal.
2. Centrifuge the fixed sample and aspirate away the ethanol.
3. Resuspend in 1 mL wash buffer that contains the same percentage formamide as the hybridization buffer you will be using. Let stand for 2–5 min.
4. Centrifuge sample and aspirate wash buffer, then add hybridization solution. Incubate in the dark overnight at 30 °C.



5. In the morning, add 1 mL of wash buffer to the sample, vortex, centrifuge, and aspirate, then resuspend in another 1 mL of wash buffer and incubate at 30 °C for 30 min.
6. Vortex, centrifuge, and aspirate the wash buffer, then resuspend in another 1 mL of wash buffer containing 5 ng/mL DAPI for nuclear counterstaining. Incubate at 30 °C for 30 min.
7. If you are imaging without using glox antifade solution (e.g., if you are using TMR), then just resuspend in an appropriate volume (>0.1 mL) of 2× SSC and proceed to imaging.
8. If you are imaging with the glox antifade solution, aspirate the buffer and resuspend in the glox buffer without enzymes for equilibration; incubate for 1–2 min.
9. Aspirate the buffer and resuspend in the 100  $\mu$ L of glox buffer to which the enzymes (glox and catalase) have been added. Proceed to imaging.

#### 4.2.2. Hybridization for samples adhered to coverglass

1. Prepare the hybridization solution: to 100  $\mu$ L of hybridization buffer, add 1–3  $\mu$ L of probe at the appropriate concentration, then vortex and centrifuge.
  - a. Be sure to warm the hybridization solution to room temperature before opening it.
  - b. For the initial test of a set of probes, it is best to start four separate hybridization reactions by adding 1  $\mu$ L each of the 1:10, 1:20, 1:50, and 1:100 working dilutions of probes to see which one is optimal.
2. Aspirate the 70% ethanol off of the sample.
3. Add 1 mL wash buffer that contains the same percentage formamide as the hybridization buffer you will be using. Let stand for 2–5 min.
4. Aspirate wash buffer and then add hybridization solution. Place a carefully cleaned coverslip over the sample to prevent drying of the hybridization solution during the incubation. Incubate in the dark overnight at 30 °C. *Note:* if using perfusion chambers on a coverslip containing a tissue section, one can remove the perfusion chamber before performing the hybridization.
5. In the morning, add 1 mL of wash buffer to the sample, remove the coverslip, then incubate at 30 °C for 30 min.
  - a. Be sure to remove the coverslip very carefully so as not to disturb the cells underneath very much.
  - b. For tissue sections, add 100  $\mu$ L wash buffer to the edges of the coverslip and gently remove the coverslip. Then reattach a perfusion chamber and proceed as usual.
6. Aspirate the wash buffer, then resuspend in another 1 mL of wash buffer containing 5 ng/mL DAPI for nuclear counterstaining. Incubate at 30 °C for 30 min.

7. If you are imaging without using glox antifade solution (e.g., if you are using TMR), then just add 1 mL of  $2\times$  SSC and proceed to imaging.
8. If you are imaging with the glox antifade solution, aspirate the buffer and resuspend in  $2\times$  SSC.
9. Aspirate the SSC and add the glox buffer without enzymes for equilibration; incubate for 1–2 min.
10. Aspirate the buffer and resuspend in the 100  $\mu$ L of glox buffer to which the enzymes (glox and catalase) have been added.
11. Place a carefully cleaned coverslip over the sample. This will spread the glox buffer over the entire sample and also slow evaporation.
12. Proceed to imaging.



## 5. IMAGING

At this point, the samples are essentially ready for imaging. The microscopy equipment required is fairly standard.

### 5.1. Microscopy equipment

1. Standard widefield fluorescence microscope (e.g., Nikon TE2000 or Ti, Zeiss Axiovert).
2. Strong light source, such as a mercury or metal-halide lamp (e.g., ExFo Excite, Prior Lumen 200). We have found that the metal-halide lamps are generally brighter, especially for the far red dyes such as Cy5.
3. Filter sets appropriate for the fluorophores chosen (see [Table 17.1](#)).
4. Standard cooled CCD camera, ideally optimized for low-light level imaging rather than speed (13  $\mu$ m pixel size or less is ideal; for example, Pixis, Princeton Instruments, CoolSNAP HQ). We have found that EMCCDs do not provide any additional signal-to-noise benefits over nongain amplified cameras.
5. High NA ( $>1.3$ )  $100\times$  DIC objective (be sure to check transmission properties when using far red dyes such as Cy5 or Cy5.5). We have also seen spots using an oil-immersion  $60\times$  objective, but the reduced spatial resolution makes the spots somewhat more difficult to identify computationally.

Generally speaking, the imaging of single mRNAs using a widefield fluorescence microscope is relatively straightforward; see [Fig. 17.4](#) for some examples. The only difference between this and many more standard applications of fluorescence microscopy is that the signals are much weaker than, say, a DAPI stain, thus requiring exposure times on the order of 2–3 s. We have found that widefield microscopy works best due to the relatively

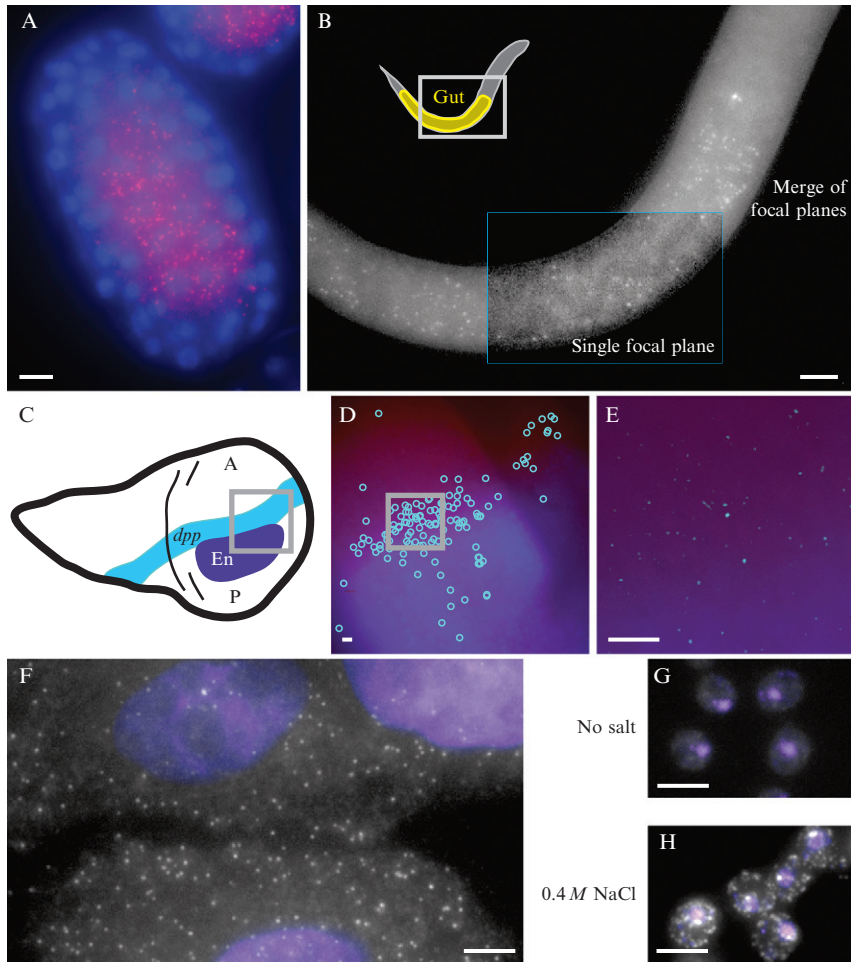


**Figure 17.4** Imaging mRNAs in a variety of biological samples. (A) *elt-2* mRNA molecules (red) in an early stage embryo (~100 cell stage) from *C. elegans*; the nuclei have been counterstained with DAPI (blue). (B) *elt-2* mRNA molecules in an L1 larva from *C. elegans*. Inside the blue box, a single focal plane is shown in which the intestinal track is visible. (C) A schematic depiction of *dpp* and *engrailed* expression in the imaginal wing discs of third instar larvae from *D. melanogaster*. (D) Image showing the locations of the computationally identified *dpp* mRNA molecules (light blue circles) and Engrailed expression detected by immunofluorescence (dark blue). (E) Image containing enhanced *dpp* mRNA molecule signals (light blue) and Engrailed protein expression detected by immunofluorescence (dark blue). (F) Image of FKBP5 mRNAs in human carcinoma cell line A549 induced with dexamethasone (nuclei in purple). (G–H) STL1 mRNA particles in both unperturbed cells (G) and cells subjected to a 10-min 0.4 M NaCl salt shock (H), with nuclear DAPI counterstaining in purple. STL1 is one among a number of yeast genes whose expression is significantly upregulated by the addition of salt to the growth medium. All images except the boxed portion of (B) are maximum merges of a *z*-stack of fluorescent images, and all scale bars are 5  $\mu$ m long.

large amount of light gathered as compared to confocal imaging setups. That said, we have had some success using both spinning disk and laser scanning confocal microscopes, but it seems that one issue with their use is that the high intensity of the laser excitation rapidly bleaches samples. Since the total light collection is much lower than in a widefield microscope (per illumination), this bleaching limits the signal one can gather and is especially problematic when one takes multiple  $z$  sections to generate three-dimensional image stacks.

However, the use of widefield microscopy places a tight limitation upon the thickness of the sample one can image, because thicker samples lead to far more out-of-focus light that can obscure the relatively faint mRNA signals. We have found that the single mRNA signals are most readily detectable when the sample is less than 7–8 microns thick. Some samples (notably *C. elegans* embryos and larvae) are considerably thicker than this limit, so we generally flatten them between two coverslips to reduce the  $z$ -extent of the sample considerably before imaging. For other samples, such as tissue sections and cell lines, the specimens are already sufficiently thin so as to obviate the requirement for flattening. Also, for imaging multiple slices, we recommend using at least a 0.2- $\mu\text{m}$   $z$  spacing between sections, and larger spacings such as 0.3 or even 0.4  $\mu\text{m}$  are also probably fine. The main consideration is an empirical one: Aim for each RNA spot showing up in at least two adjacent optical sections. This gives confidence that the spots identified are legitimate.

There are also some common microscopy practices that one should avoid when doing single molecule FISH. One of these is the use of commercial antifade mounting media. We have found that while these media do decrease the rate of photobleaching, they also lower the overall fluorescence of the sample and also introduce a strong background that interferes with the FISH signals (most likely from the glycerol included in many of these solutions). We recommend avoiding these entirely and just imaging with the antifade glox solution (or just 2 $\times$  SSC if photobleaching is not a concern). Another thing to avoid is the use of nail polish to seal samples. This introduces a high background into the sample, again obscuring the FISH signals. We recommend sealing with silicone-based vacuum grease instead.

Regarding the mounting of the samples, we use #1 coverglass to image all of our samples. We have found that our signals are better with #1 than with #1.5, even though our objectives (like most) are designed for use with #1.5 coverglass. Also, one should avoid having ones samples on a microscopy slide and then “covering” them with coverglass. We have found that the subsequent layer of liquid between the top of the coverglass and the sample causes the signals to blur.

If the target RNAs are stained properly, you will see clear diffraction-limited spots, such as those depicted in [Fig. 17.4](#). The width of the spots is

roughly 200–500 nm, depending on the dye and the imaging setup. While the intensities of the individual spots may vary, the spot size should be essentially identical. (An exception to this are active sites of transcription, at which many nascent mRNAs accumulate, resulting in a somewhat larger and significantly brighter spot (Femino *et al.*, 1998; Raj *et al.*, 2006; Vargas *et al.*, 2005) Variability in the spot size is an indication that the spots are not actually target mRNAs but rather are some form of autofluorescent background. One way to check for this is to perform the hybridization without adding the probes to check if the allegedly nonspecific spots persist. Another way to see if the spots are merely autofluorescent background is to acquire images with different filter sets. Typically, the autofluorescent background will show up in multiple channels, owing to the rather broad spectral properties of cellular autofluorescence—with appropriate filters, there is essentially no bleedthrough between the different organic dyes used to label the oligonucleotides (Fig. 17.3) (Raj *et al.*, 2008).

## 6. IMAGE ANALYSIS

The analysis of images acquired using this method involves the computer-assisted identification of spots in a three-dimensional set of images (Fig. 17.5). Given that the spot-like signals are significantly brighter than the background, one might assume that a simple threshold would be sufficient. Unfortunately, due to out-of-focus light, the background itself often varies greatly throughout the image, making the simple application of a threshold impossible. To remove this (typically slowly varying) background, we employ Laplacian of Gaussian (LoG) filters (Fig. 17.5B). The LoG filter has essentially one parameter, which is the width of the filter. For any particular microscope/camera combination, we usually determine the optimal filter width by trial and error (theoretically, the width of the filter should be the same as the width of the spots one is trying to identify). We should note that we apply our filters in three-dimensions, thus using the three-dimensionality of the spots to further enhance the signals.

Another option for removing the out-of-focus light is deconvolution software. We have found, though, that while the results from deconvolution are often nice, they seldom yield results that are better in terms of spot counting accuracy. Moreover, they are extremely expensive, both monetarily and computationally. For these reasons, we find our simple linear filtering approach to be more appropriate, especially for large data sets.

After performing the filtering, one must select an appropriate threshold. We have found that this task is difficult to automate, since it is difficult to say *a priori* what the appropriate threshold is. Instead, we compute the number of spots detected for all possible thresholds. Upon graphing this relationship,

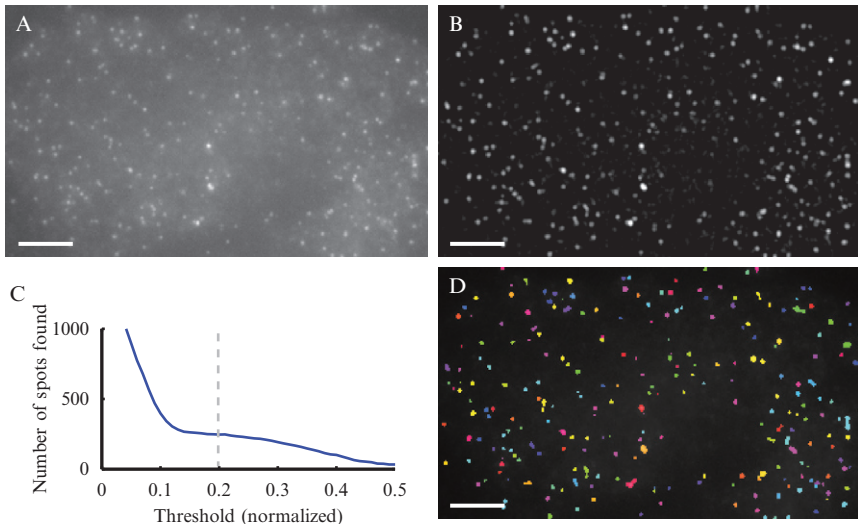


**Figure 17.5** Computational identification of mRNA spots. (A) Raw image data (maximum intensity merge) obtained from imaging FKBP5 mRNA particles in A549 cells induced with dexamethasone. (B) Image (maximum merge) obtained by running raw data through Laplacian of a Gaussian filter designed to enhance spots of the correct size and shape while removing the slowly varying background. (C) The number of spots (i.e., connected components) found upon thresholding the filtered image from (B) is plotted as a function of the threshold value, ranging from 0 to the maximum intensity of the filtered image (normalized to 1). The presence of a plateau indicates that there is a region over which the number of particles detected is fairly insensitive to the particular threshold chosen. The gray line represents the threshold used (within the plateau) for determining the actual number of mRNA in the image. (D) Image showing the results of using the threshold represented by the gray line in C on the filtered image in (B), with each distinct spot assigned a random color. The spots detected correspond very well with those identified by eye. All scale bars are 5  $\mu\text{m}$  long. Adapted with permission from Supplementary Fig. 1 of [Raj \*et al.\* \(2008\)](#).

we found that there was a plateau region in the graph, which means that there is a broad region of thresholds over which the spot count does not vary significantly ([Fig. 17.5C](#)). This is generally the correct threshold to choose, as spots identified at those thresholds correspond nicely to those identified by eye ([Fig. 17.5D](#)). Our image processing pipeline is thus to first preprocess the data via filtering and applying all possible thresholds, then manually picking thresholds based on the graph (with some visual feedback). We find that this facilitates rapid processing of many images, allowing one to threshold hundreds of images in a matter of hours.

Software demonstrating these algorithms (implemented in MATLAB and including some sample data) is free for download at: [http://rajlab.seas.upenn.edu/pdfs/raj\\_nat\\_meth\\_2008\\_software.zip](http://rajlab.seas.upenn.edu/pdfs/raj_nat_meth_2008_software.zip).

## ACKNOWLEDGMENTS

Sanjay Tyagi acknowledges support from National Institutes of Health grant NIMH-079197. Arjun Raj acknowledges support from National Science Foundation postdoctoral fellowship DMS-0603392 and a Burroughs-Wellcome Fund Career Award at the Scientific Interface.

## REFERENCES

- Femino, A. M., Fay, F. S., Fogarty, K., and Singer, R. H. (1998). Visualization of single RNA transcripts in situ. *Science* **280**, 585–590.
- Gall, J. G. (1968). Differential synthesis of the genes for ribosomal RNA during amphibian oögenesis. *Proc. Natl. Acad. Sci. USA* **60**, 553–560.
- Golding, I., Paulsson, J., Zawilski, S. M., and Cox, E. C. (2005). Real-time kinetics of gene activity in individual bacteria. *Cell* **123**, 1025–1036.
- Larson, D. R., Singer, R. H., and Zenklusen, D. (2009). A single molecule view of gene expression. *Trends Cell Biol.* **19**, 630–637.
- Levsky, J. M., and Singer, D. (2003). Fluorescence in situ hybridization: Past, present and future. *J. Cell Sci.* **116**, 2833–2838.
- Maamar, H., Raj, A., and Dubnau, D. (2007). Noise in gene expression determines cell fate in *Bacillus subtilis*. *Science* **317**, 526–529.
- Maheshri, N., and O'shea, E. K. (2007). Living with noisy genes: How cells function reliably with inherent variability in gene expression. *Ann. Rev. Biophys. Biomol. Struct.* **36**, 413–434.
- Raap, A. K., Van de corput, M. P., Vervenne, R. A., Van gijlswijk, R. P., Tanke, H. J., and Wiegant, J. (1995). Ultra-sensitive FISH using peroxidase-mediated deposition of biotin- or fluorochrome tyramides. *Hum. Mol. Genet.* **4**, 529–534.
- Raj, A., and Van oudenaarden, A. (2008). Nature, nurture, or chance: Stochastic gene expression and its consequences. *Cell* **135**, 216–226.
- Raj, A., and Van oudenaarden, A. (2009). Single-molecule approaches to stochastic gene expression. *Ann. Rev. Biophys.* **38**, 255–270.
- Raj, A., Peskin, C. S., Tranchina, D., Vargas, D. Y., and Tyagi, S. (2006). Stochastic mRNA synthesis in mammalian cells. *PLoS Biol.* **4**, e309.
- Raj, A., Van den bogaard, P., Rifkin, S. A., Van oudenaarden, A., and Tyagi, S. (2008). Imaging individual mRNA molecules using multiple singly labeled probes. *Nat. Methods* **5**, 877–879.
- Tautz, D., and Pfeifle, C. (1989). A non-radioactive in situ hybridization method for the localization of specific RNAs in *Drosophila* embryos reveals translational control of the segmentation gene hunchback. *Chromosoma* **98**, 81–85.
- Vargas, D. Y., Raj, A., Marras, S. A., Kramer, F. R., and Tyagi, S. (2005). Mechanism of mRNA transport in the nucleus. *Proc. Natl. Acad. Sci. USA* **102**, 17008–17013.
- Yildiz, A., Forkey, J. N., McKinney, S. A., Ha, T., Goldman, Y. E., and Selvin, P. R. (2003). Myosin V walks hand-over-hand: Single fluorophore imaging with 1.5-nm localization. *Science* **300**, 2061–2065.
- Zenklusen, D., Larson, D. R., and Singer, R. H. (2008). Single-RNA counting reveals alternative modes of gene expression in yeast. *Nat. Struct. Mol. Biol.* **15**, 1263–1271.